DOI: 10.1177/0956797614532656

Supplementary materials:

The color-diversity relation between the cued and of the non-cued rows:

Over the course of Exp.1 the relation between color-diversity of the cued-row and non-cued rows was manipulated in the following manner (see also figure S1): in block-1 (the first 100 trials) both the cued and the non-cued rows had an identical color-diversity level ('congruent'). In the next 150 trials, the color-diversities were independent of each other ('orthogonal'). Over the next 120 trials, the color-diversity levels were always opposite ('incongruent'). In block 2, (190 final trials of Exp.1) the color-diversities of the cued-row and the non-cued rows varied independently (as in the orthogonal trials). In all trials in Exp.2-6 the color-diversities were independent of each other (orthogonal).

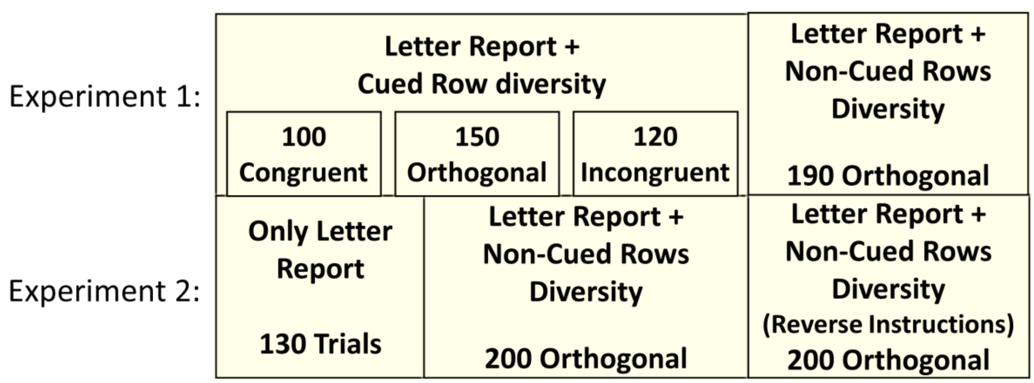

Figure S1: The different trial-types in exp.1 and 2

Dependent variable for letter-recall - WM-capacity:

To calculate the amount of items maintained in participants' working memory, we corrected participants' accuracy in the letter-report task for guessing responses in the following manner:

DOI: 10.1177/0956797614532656

$$M = \frac{N(C \cdot A - 1)}{(C - 1)} \quad .$$

Where *N* is the number of presented items (in our design - 6 letters), *C* is the number of response alternatives (9) and *A* is the observed accuracy. We assume that subjects remember M out of N letters and guess the rest ($N - M$). Each correct response contributes $1/N$ to the total accuracy. If subjects remember a letter, the probability of a correct response will be 1; if they guess between C alternatives, the probability of it being a correct guess $1/C$. The expected accuracy A is therefore given by:

$$A = \sum_{M} \left(\frac{1}{N}\right)(1) + \sum_{N-M} \left(\frac{1}{N}\right)\left(\frac{1}{C}\right) = \frac{MC + N - M}{NC}$$

The colors used:

We used 19 possible colors – pink, violetred, orchid, mediumorchid, purple, slateblue, blue, royalblue, steelblue, turquoise, spring-green, green, olive-drab, yellow, gold, orange, sienna, orange-red and red.

Exp.3 (N=9) Method:

We used 6 random hues (ranging the entire color wheel) for creating the low-diversity condition and introduced colorless catch-trials (Fig. S2).

DOI: 10.1177/0956797614532656

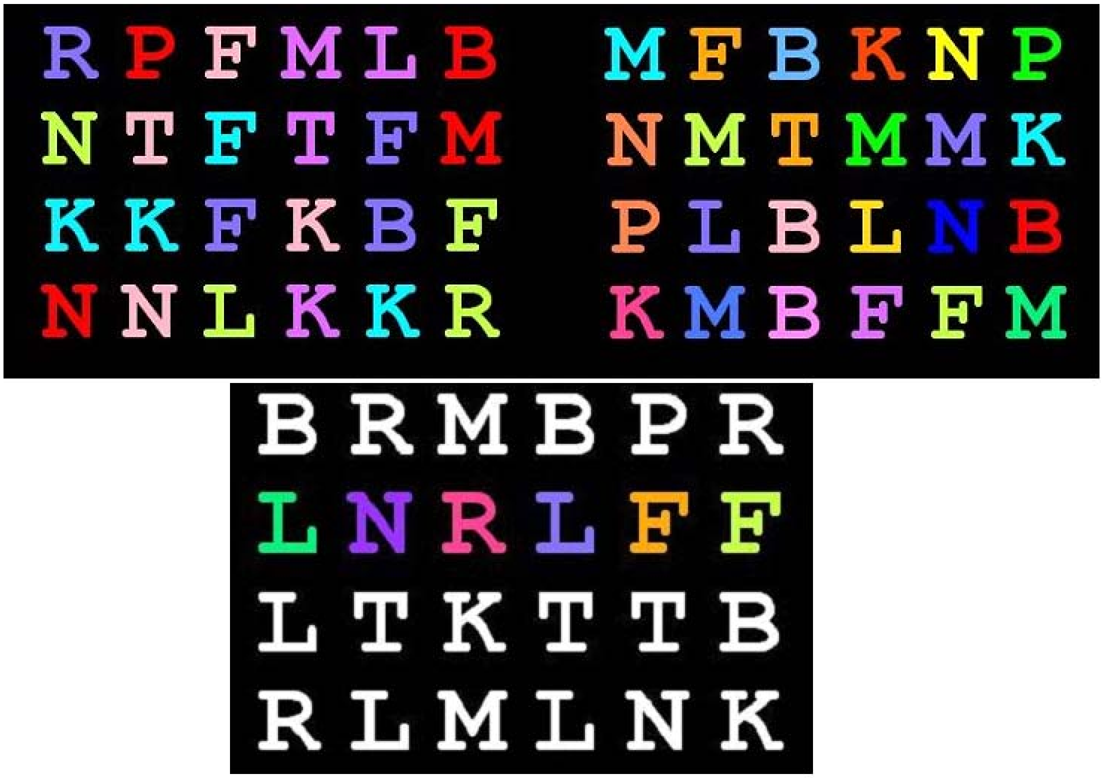

Figure S2. Low (top left panel) and high (top right) 'complexity' levels; below: a sample of a 'catch' trail

Exp.4 (N=6) Method:

Experiment-4 was identical to Experiment-2 except that on each trial, immediately at the offset of the letter-array, 300ms Mondrian-masks (3X100ms) were presented (i.e., no blank interval between the letter array and the mask; see Fig. S3). Following the mask, participant either reported only the cued letter (block 1) or also made color-diversity judgment (block 2).

DOI: 10.1177/0956797614532656

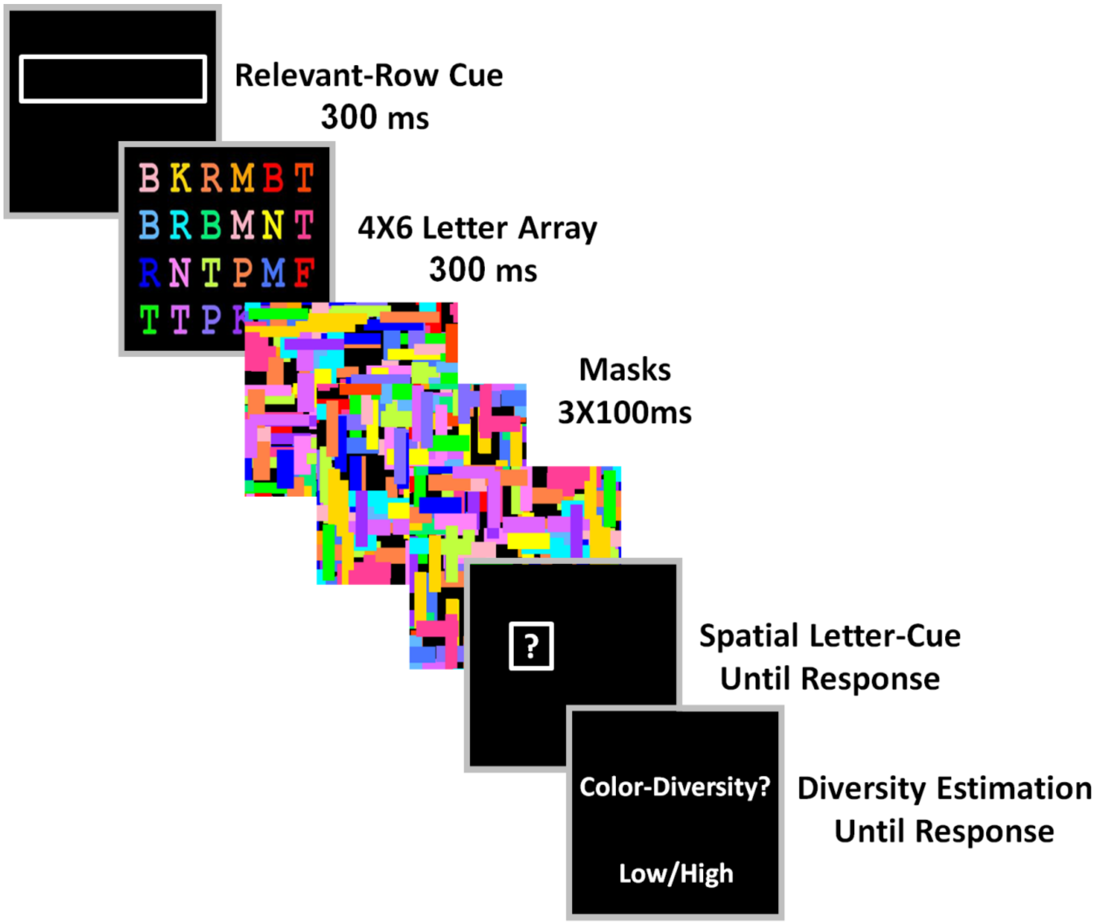

Figure S3. Time line illustration of a single trial in Exp.4

Exp.6 (N=13) Method:

Experiment-6 was identical to Experiment-5 except that the letter-array was presented for 10 ms (instead of 16.7 ms) and the ISIs were either 0, 10, 20, 30 or 40 ms. Instead of displaying low or high color-diversity, we used red and blue colored letters and tested the ability to detect the dominant color (16/24 of letters were either blue or red randomly between trials; Fig.S4).

DOI: 10.1177/0956797614532656

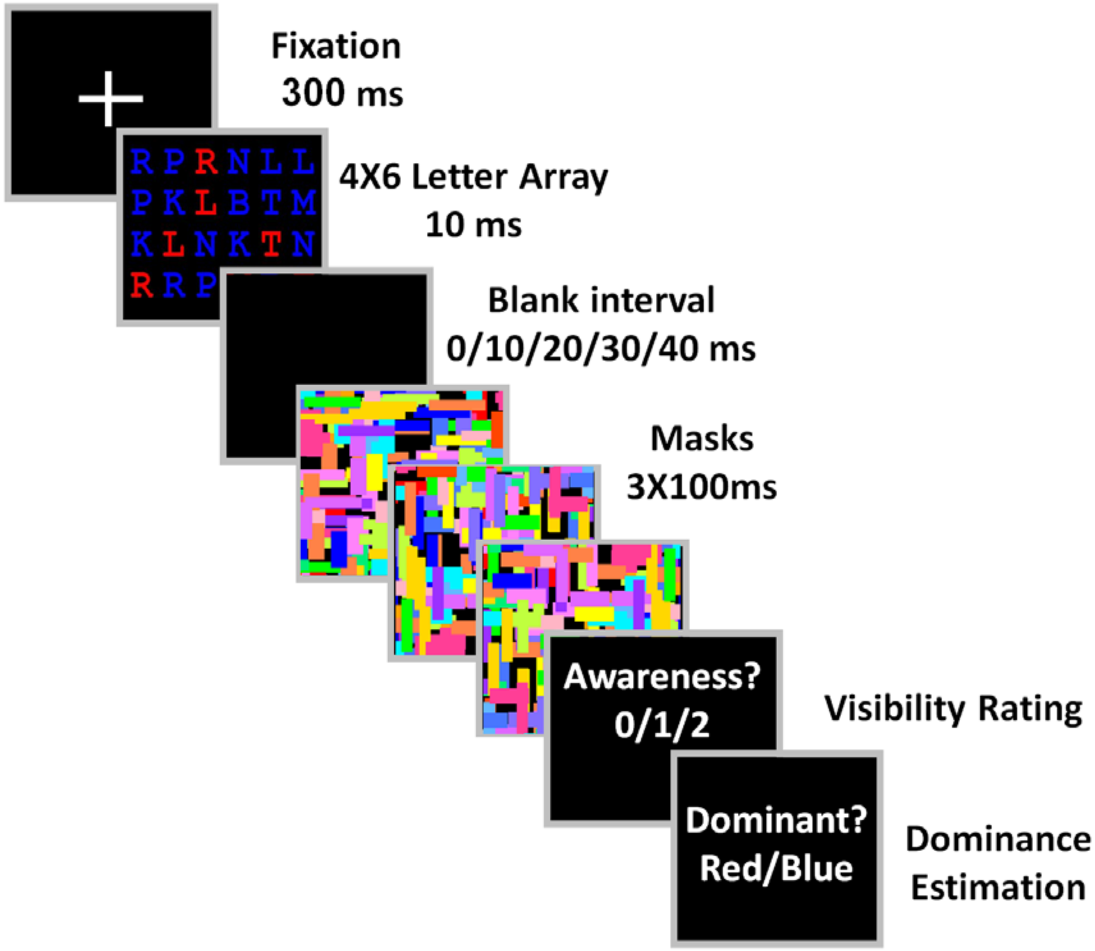

Figure S4. Time-line illustration of a 'blue' trial in Exp.6

WMC results:

WMC was not affected by the color-diversity relations between the cued and the non-cued rows (Exp.1; WMC_congruent=3; WMC_orthogonal=3.2; WMC_incongruent=3.1; WM_non-cued=3.2; repeated measures ANOVA $F(3,30)=0.44$; $p = 0.73$; see figure S5).

DOI: 10.1177/0956797614532656

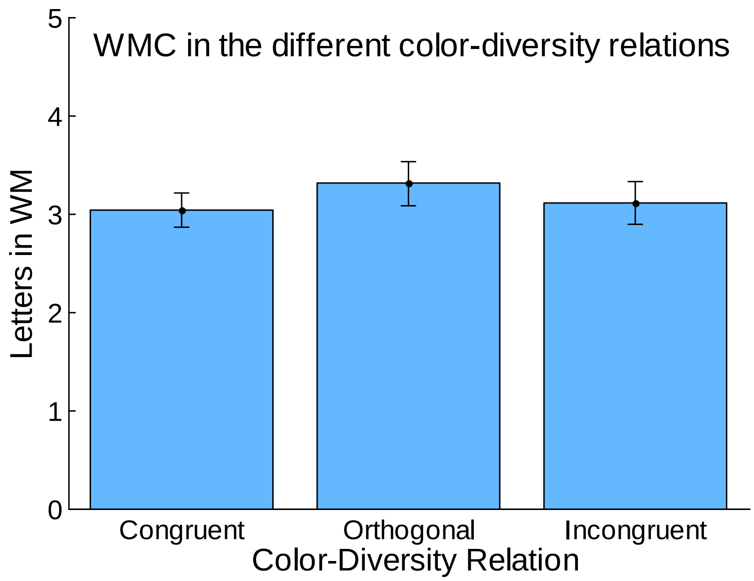

Figure S5 - WMC between the different diversity relations when participants had to estimate the cued row's diversity level. Error bars denote 1 SEM.

Likewise, WMC did not vary between congruent and incongruent trials when participants estimated the color-diversity level of the non-cued rows [Exp.1: WMC_Cong=3.23; WMC_Incong=3.09; t(11)=1.32 ; p=0.22. Exp.2: WMC_Cong=3.04; WMC_Incong=3.12; t(11)=-0.71; p=0.5]. In addition, WMC did not differ between letter-only trials and color-diversity trials in Exp.3 and 4 [Exp.3: WMC_Letters=2.06; WMC_Diversity=2.23; t(8)=-1.3; p=0.23; Exp.4: WMC_Letters=2.11; WMC_ Diversity =2.17; t(5)=-0.3; p=0.78].

Color-diversity sensitivity:

Participants exhibited above-chance sensitivity to the color-diversity of the non-cued rows [Exp.2: M_Accuracy=65%; t(8)=5.48, as compared to chance; p=0.0006; see figure S6; Exp.3: M_Accuracy=61%; t(8)=4.3, as compared to chance; p=0.003: Exp.4: M_Accuracy=63%; t(5)=2.82, compared to 50%; p=0.04].

DOI: 10.1177/0956797614532656

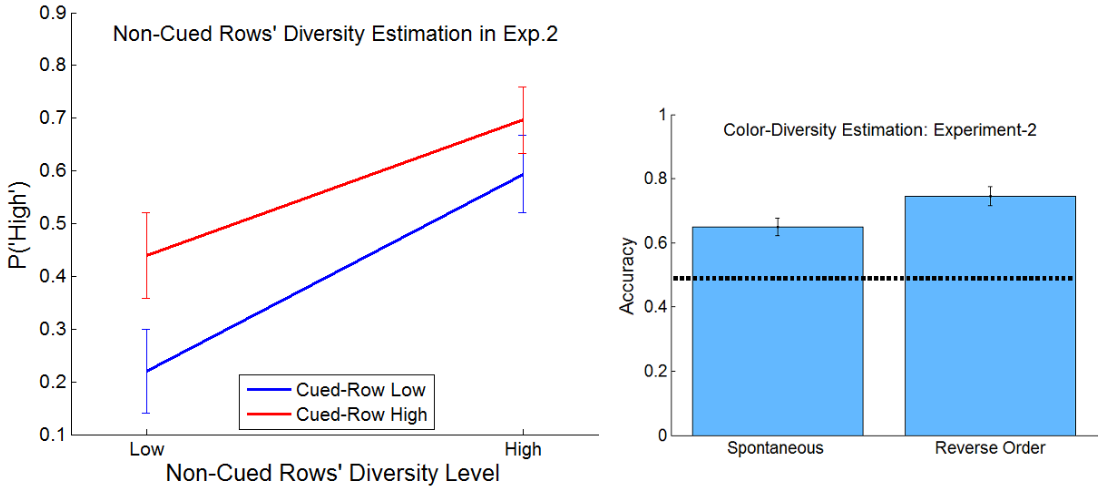

Figure S6 – Color-diversity accuracy in exp.2; Error bars denote 1 SEM.

Sensitivity to catch-trials in Exp. 3

Overall, 56 of the 90 catch trials (10 trials per subject) were correctly identified as such [M_Catch=62%; t(8)=3.98, as compared to 0; p=0.004; no false alarms].

Exp.6 Results:

We employed the exact analysis as in Exp.5 and observed above-chance performance when participants reported no conscious experience of the colors [M_Accuracy=54.9%; t(12)=-3.16, as compared to 50%; p=0.009]. Likewise above-chance performance was observed specifically in the unseen trials under the 20 ms ISI [M_Accuracy=62.93%; t(12)=5.75, as compared to 50%; p<0.001; see Fig S.7].

DOI: 10.1177/0956797614532656

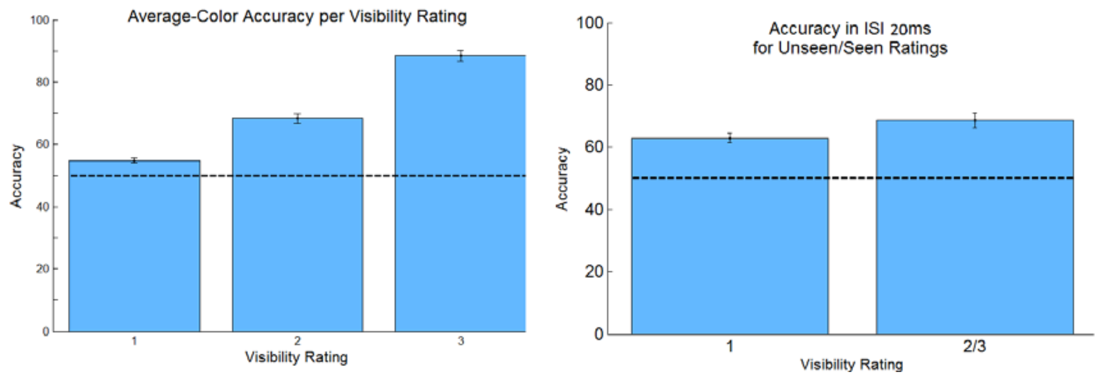

Figure S7. Unconscious color-processing in Exp.6; accuracy per visibility rating (left) and accuracy per visibility-rating, specifically in the ISI=20ms trials; dashed line indicates chance performance and Error bars denote 1 SEM.

Simulation study: discrimination of average-color and color-diversity, as a function of the items' color distinctiveness.

Simulation-1. Conceptual/abstract model

We carried out a simulation model to test whether an accurate color-diversity computation is, in principle, possible on the basis of highly degraded color representations of the individual letters. In other words, we are asking if it is possible to compute color-diversity to the degree needed for carrying out the high/low color-diversity task, without having perceived the individual colors. We operationalize low color-perception as involving a blurry or noisy representation of the individual colors. We expected that while averaging across color-elements via a population code would result in a robust estimation of the actual average color (since the noise at the specific elements would average out), the estimation of the color-diversity would not be robust to noise.

DOI: 10.1177/0956797614532656

To show this, we simulated 1000 trials (500 of high-diversity and 500 of low-diversity), whereby on each trial 18 colors (corresponding to the amount of non-cued letters in our experiments) were generated by sampling each color either from the whole range of 21 colors (high diversity), or from a restricted range of 7 *adjacent colors* (low diversity). For simplicity we assume here that each color is represented by a numerical value from 1-21 (this ignores the cyclic nature of our color space, but the results are unaffected by this). To “manipulate” low (or blurry) color-perception, we perturbed each color sample, by adding to it with a Gaussian variable (this may correspond to the ‘winning’ noisy color filter that responds best to the specific color; see Simulation-2 for an demonstration of this mechanism). For each level of the noise parameter (the standard deviation of the Gaussian bell), we calculated 3 measurements:

i) the accuracy in identifying the color of a single-item – this was strongly affected by noise, as per the assumption (Fig. S5, cyan line).

ii) the accuracy in identifying the average color of the entire display – this was expected to be noise-robust, as confirmed by the simulation result (Fig. S5, red line).

iii) the accuracy in estimating the color diversity in the display – whose degree of robustness is under question. Does color-diversity behave more like the cyan or the red line, above? The results clearly confirm our expectation: unlike the average color, the color-diversity is not robust to noise/perceptual degradation (Fig S5, blue line).

DOI: 10.1177/0956797614532656

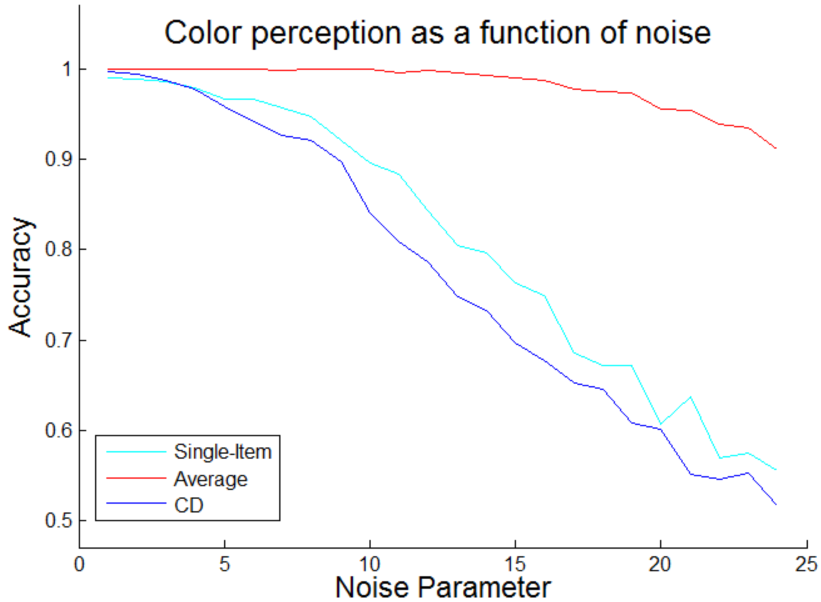

Figure S7 – a simulation-based analysis of accuracy in estimating the color of a single item (cyan), of the items' average color (red) and of items' color diversity (blue) as a function of perceptual noise. The single-item accuracy was calculated as the fraction of trials in which the single item's perturbed color was in a +/- 5 adjacent colors range (half of the entire range) as compared to the actual single-items' color. The accuracy of average-color was calculated as the fraction of trials in which the average of the 18 perturbed colors was in a +/- 5 adjacent colors range as compared to the actual 18-item color-average. The precision range (-5,5) was chosen to obtain a binary decision (with same chance-level baseline) as for the color-diversity *estimation. The simulated* color-diversity *estimation was computed by comparing the SD of the values of the 18 samples, with the mean of that SD across all the 1000 trials (including both high/low diversities). Note that this is an ideal observer analysis.*

Simulation-2: a neural coding model

DOI: 10.1177/0956797614532656

We ran a second simulation to demonstrate the sensitivity of color-diversity estimation to degradation in the colors' representation, within a neural coding model. For each letter, we represent the color with a population of 24 color-units, that optimally tuned to colors around the color-circle (Fig. 1A), at a resolution of 15 deg (360/24). Each detector has a Gaussian tuning on the circular/periodic space, whose SD corresponds to the degree of color degradation (sharp vs. blurred; see Fig.S6).

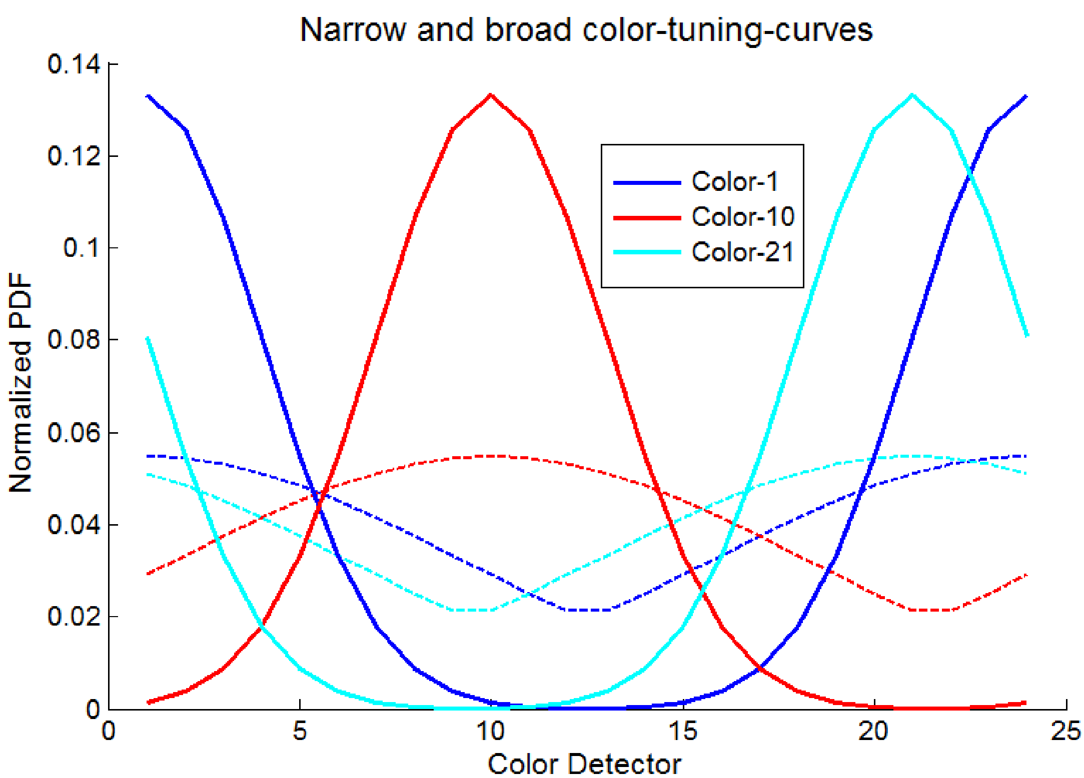

Figure S8 - periodic color-tuning-curves of colors 1, 10 and 21 for low perceptual noise (SD=3; filled lines) and high perceptual noise (SD=8; dashed lines). The tuning curves are normalized to 1.

DOI: 10.1177/0956797614532656

Upon the presentation of a specific color, all 24 detectors at that locations respond probabilistically, by triggering a number of spikes, that distributed according to a Poisson statistics with a rate, lambda, proportional to the tuning-curve above. In this simulation the proportionality constant is 100.

$$f(k;\lambda) = \Pr(X=k) = \frac{e^{-\lambda}\lambda^{k}}{k!}$$

Thus, for each ‘presented’ item, we obtained a noisy ‘activation profile’ of the entire population. We then generated 10000 trials, where on each trial 18 colors were sampled either from 24 color possibilities (high diversity), or from 8 possibilities (low diversity). We simulated for each trial, the populations’ activity in response to each of the 18 colors presented. For each presented color, the detector with the maximum activity was chosen as the ‘perceived’ item – the best guess. We illustrate this in Fig. S7, which shows a histogram for the best guess to 10,000 trials in which color-7 was presented for two level of degradation: moderate and high.

DOI: 10.1177/0956797614532656

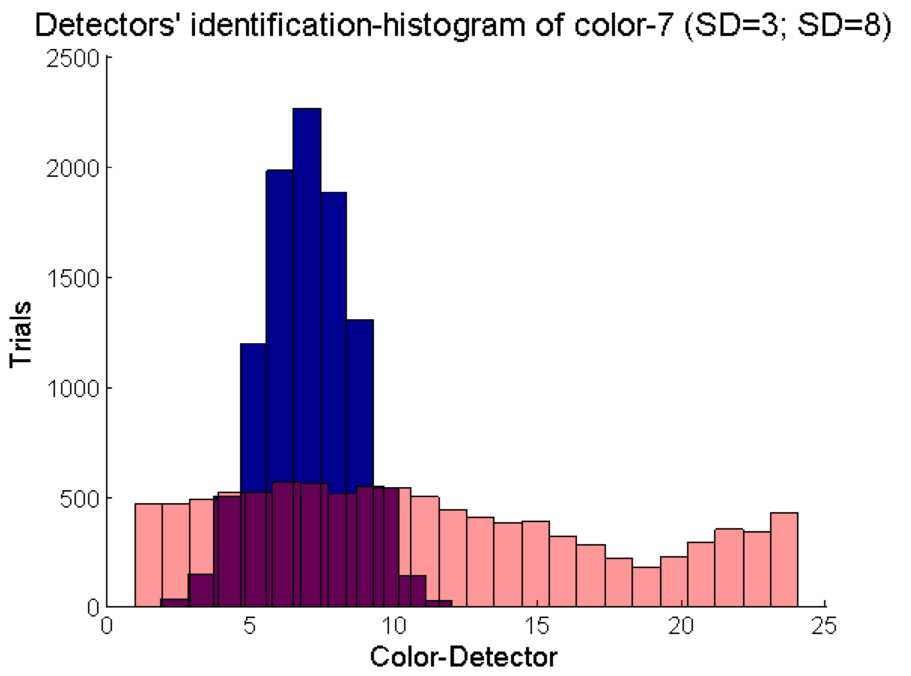

Figure S9 - Simulation-2: histograms for the best guess across 10,000 trials in which color-7 was presented for two level of degradation: moderate (SD=3; blue) and high (SD=8; pink)

We next compute, as in Simulation-1, the accuracy in I) single-color discrimination, ii) the accuracy in average color discrimination, iii) the color-diversity accuracy. The resolution was chosen to have all 3 measures have the same chance-level.

Specially, to determine single-item accuracy, we chose one of the presented items and calculated the fraction of trials in which the detector with the maximum activity in the population did not differ in more than 90□ from the actual selected color. In order to determine average-color accuracy, we first calculated, for each trial, the absolute (circular) distances between each of the 'perceived' colors (the maximal activity detector, per single-item) and the actual item-color. Average-color accuracy was calculated as the fraction of trials in which the average absolute distance was below 90. Finally, in order to calculate color -diversity accuracy, we first calculated, for each simulated trial, the sum of all the absolute (circular) distances described above, and calculated the fraction of trials in which the trial-specific sum was below the overall mean of sums across trials. Again we use the ideal observer assumptions. The results are shown in Figure S8, and are consistent with the ones obtained in the conceptual model.

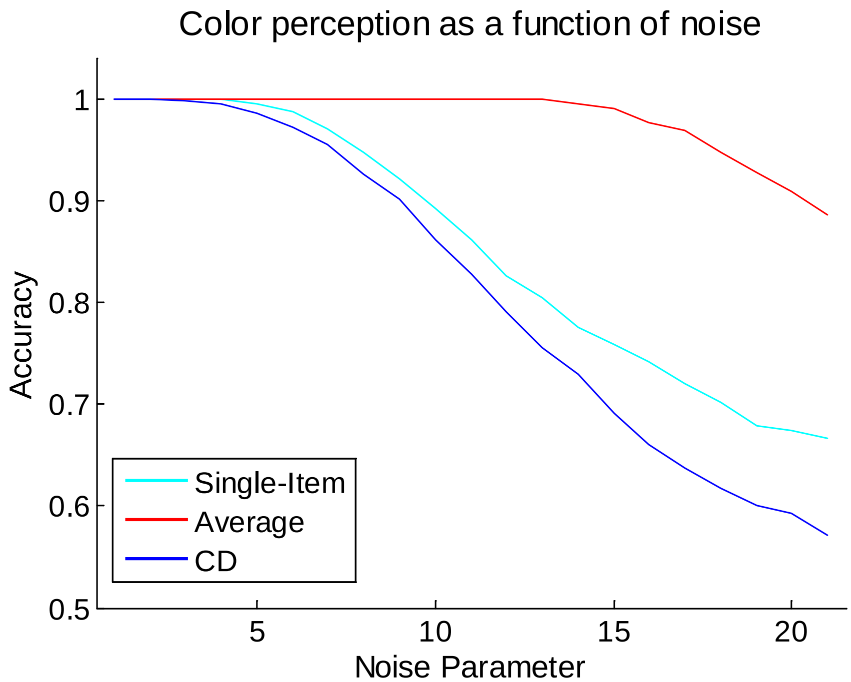

Figure S10 – Simulation-2 results of accuracy as a function of perceptual noise in single-item color estimation (cyan), average-color estimation (red) and color-diversity estimation (blue); the noise parameter is the 0.5 STD of the Gaussian tuning curves

Taken together, these computational studies suggest that much like the identification of a single items' color and unlike the estimations of the average-color, above-chance estimations of color-diversity must rely on a relatively high ratio of signal to noise at the perceptual level.